

Inhibition of STAT3 Signaling Reduces IgA1 Autoantigen Production in IgA Nephropathy



Koshi Yamada^{1,4}, Zhi-Qiang Huang^{1,9}, Milan Raska^{1,5,9}, Colin Reily^{3,9}, Joshua C. Anderson², Hitoshi Suzuki^{1,4}, Hiroyuki Ueda¹, Zina Moldoveanu¹, Krzysztof Kiryluk⁶, Yusuke Suzuki⁴, Robert J. Wyatt⁷, Yasuhiko Tomino^{4,8}, Ali G. Gharavi⁶, Amy Weinmann¹, Bruce A. Julian^{1,3}, Christopher D. Willey² and Jan Novak¹

¹Department of Microbiology, University of Alabama at Birmingham, Birmingham, Alabama, USA; ²Department of Radiation Oncology, University of Alabama at Birmingham, Birmingham, Alabama, USA; ³Department of Medicine, University of Alabama at Birmingham, Birmingham, Alabama, USA; ⁴Division of Nephrology, Department of Internal Medicine, Juntendo University Faculty of Medicine, Tokyo, Japan; ⁵Department of Immunology, Faculty of Medicine and Dentistry, Palacky University and University Hospital Olomouc, Olomouc, Czech Republic; ⁶Department of Medicine, College of Physicians and Surgeons, Columbia University, New York, USA; ⁷Department of Pediatrics, University of Tennessee Health Center, Memphis, Tennessee, USA; and ⁸Medical Corporation Showakai, Tokyo, Japan

Introduction: IgA nephropathy is a chronic renal disease characterized by mesangial immunodeposits that contain autoantigen, which is aberrantly glycosylated IgA1 with some hinge-region *O*-glycans deficient in galactose. Macroscopic hematuria during an upper respiratory tract infection is common among patients with IgA nephropathy, which suggests a connection between inflammation and disease activity. Interleukin-6 (IL-6) is an inflammatory cytokine involved in IgA immune response. We previously showed that IL-6 selectively increases production of galactose-deficient IgA1 in IgA1-secreting cells from patients with IgA nephropathy.

Methods: We characterized IL-6 signaling pathways involved in the overproduction of galactose-deficient IgA1. To understand molecular mechanisms, IL-6 signaling was analyzed by kinomic activity profiling and Western blotting, followed by confirmation assays using siRNA knock-down and small-molecule inhibitors.

Results: STAT3 was differentially activated by IL-6 in IgA1-secreting cells from patients with IgA nephropathy compared with those from healthy control subjects. Specifically, IL-6 induced enhanced and prolonged phosphorylation of STAT3 in the cells from patients with IgA nephropathy, which resulted in overproduction of galactose-deficient IgA1. This IL-6-mediated overproduction of galactose-deficient IgA1 could be blocked by small molecule inhibitors of JAK/STAT signaling.

Discussion: Our results revealed that IL-6-induced aberrant activation of STAT3-mediated overproduction of galactose-deficient IgA1. STAT3 signaling pathway may thus represent a new target for disease-specific therapy of IgA nephropathy.

Kidney Int Rep (2017) 2, 1194–1207; <http://dx.doi.org/10.1016/j.ekir.2017.07.002>

KEY WORDS: aberrant glycosylation; autoantigen; IgA1; IgA nephropathy; *O*-glycans

© 2017 International Society of Nephrology. Published by Elsevier Inc. This is an open access article under the CC BY-NC-ND license (<http://creativecommons.org/licenses/by-nc-nd/4.0/>).

IgA nephropathy (IgAN), first described by Berger and Hinglais in 1968,¹ is the most common form of primary glomerulonephritis in the world.² Up to 40% of patients progress to end-stage renal disease within 20 years of diagnosis³ because there is no disease-specific therapy. IgAN is a mesangioproliferative disease defined by the dominance or co-dominance of IgA in

the mesangial immune deposits. IgA in the mesangial deposits is in the IgA1 subclass⁴ and is enriched for IgA1, with some *O*-glycans being galactose-deficient (Gd-IgA1).^{5,6} IgAN has been characterized as an autoimmune disease, in which the IgA1-containing mesangial immunodeposits are likely derived from circulating immune complexes^{7,8} which consist of Gd-IgA1 (autoantigen) bound by Gd-IgA1-specific autoantibodies.^{9–11} Patients with IgAN have elevated serum levels of Gd-IgA1^{7,10,12–14} that are genetically co-determined.¹⁵ Serum Gd-IgA1 levels predict disease progression,¹⁶ presumably because they drive production of pathogenic immune complexes.^{17,18} Some

Correspondence: Jan Novak, Department of Microbiology, University of Alabama at Birmingham, 845 19th Street South, BBRB 761A, Birmingham, Alabama 35294, USA. E-mail: jannovak@uab.edu

⁹These authors contributed equally to this work.

Received 15 June 2017; accepted 6 July 2017; published online 18 July 2017

circulating Gd-IgA1-containing immune complexes deposit in the mesangium and then activate mesangial cells, thus initiating glomerular injury (for review, see Wyatt and Julian⁸ and Mestecky et al.¹⁹).

Clinical expression of IgAN, particularly in children and adolescents, is often characterized by macroscopic hematuria associated with infections of the upper respiratory tract²⁰ and/or the digestive system.²¹ It has therefore been proposed that the pathogenesis of IgAN may be related to abnormalities of the mucosal immune system, including the tonsils.^{22,23} Genome-wide association studies (GWAS) support these conclusions because several candidate loci contain genes involved in innate and mucosal immunity.^{24,25} It is speculated that levels of Gd-IgA1 in the circulation increase during mucosal infections.²⁶ These infections can have a substantial impact on cytokine production; for example, they result in elevated local and circulatory levels of interleukin-6 (IL-6) in IgAN patients that may subsequently affect IgA1 O-glycosylation.^{26,27}

Studies of pathogenesis of IgAN are complicated by uniqueness of the human IgA system. This uniqueness prevents studies of IgA1 O-glycosylation in experimental animals because only humans and hominoid primates have IgA1 subclass with its O-glycans. To circumvent this problem, we generated immortalized IgA1-producing cell lines from IgAN patients and healthy control subjects (HCs) as a model system for analyses of IgA1 O-glycosylation pathways.²⁸ Our studies revealed that cells from patients with IgAN secrete more Gd-IgA1 than do the cells from HCs, concordantly with the serum levels of Gd-IgA1 of the corresponding donors. The basis for production of Gd-IgA1 is abnormal expression and activity of 2 glycosyltransferases: decreased for core 1 β 1,3-galactosyltransferase (C1GalT1), which adds galactose to *N*-acetylgalactosamine (GalNAc), and elevated for α -*N*-acetylgalactosaminide α -2,6-sialyltransferase II (ST6GalNAc-II), which adds sialic acid to GalNAc.²⁸ Moreover, in cells from IgAN patients, but not HCs, IL-6 increased galactose deficiency of secreted IgA1, which was likely due to the altered expression and activity of C1GalT1 and ST6GalNAc-II enzymes.²⁶ No other tested cytokine exhibited such a striking specific effect on Gd-IgA1 production.

In this study, we sought to understand the mechanisms that regulate these abnormal responses to IL-6. We analyzed IL-6 signaling pathways using IgA1-producing cells derived from the peripheral blood of patients with IgAN and HCs. Furthermore, we generated IgA1-producing cell lines from the tonsils of patients with IgAN and individuals with obstructive sleep apnea (OSA), and we report limited exploratory

experiments with these cells as [supplementary data](#). Using kinomic approaches, siRNA knock-down, and specific protein-kinase inhibitors, we determined that abnormal IL-6 signaling through the JAK/STAT3 pathway in IgA1-producing cells was associated with elevated synthesis of Gd-IgA1 in cells from patients with IgAN. These data thus provided a mechanism that explained a cytokine-driven increased formation of immune complexes and disease exacerbation in IgAN patients during mucosal infections. Furthermore, the findings identified a potential target for disease-specific intervention of this chronic disease that would reduce production of the main autoantigen, Gd-IgA1.

MATERIALS AND METHODS

Study Design and Preparation of Epstein-Barr Virus-Immortalized IgA1-Secreting Cells

The study was designed to investigate the signaling mechanisms responsible for the IL-6-induced increase of Gd-IgA1 in IgAN. Protocols for obtaining the blood samples and tonsillar tissue for isolation of cells were approved by Institutional Review Boards of the University of Alabama at Birmingham and Juntendo University, and the samples were obtained after written informed consent was obtained from the study subjects.

Blood samples were obtained by venipuncture from 5 patients with biopsy-proven IgAN and 5 HCs.²⁸ Tonsil samples were obtained from 2 other patients with biopsy-proven IgAN and 2 individuals with OSA who had undergone tonsillectomy in Juntendo University Hospital. Tonsillar tissue samples were immediately dissected into small pieces that were mechanically dissociated on a 100- μ m cell strainer.^{29,30} Mononuclear cells from blood and tonsil tissues were isolated by the Ficoll-Hypaque density gradient, and the cell cultures were treated with cyclosporine and thereafter immortalized by infection with the Epstein-Barr virus (EBV).²⁸

IgA1-secreting cells derived from blood or tonsils were subcloned by limiting dilution.²⁸ Cells were grown in Roswell Park Memorial Institute medium 1640 supplemented with 20% fetal bovine serum, 100 U/ml of penicillin, and 0.1 mg/ml of streptomycin in a humidified carbon dioxide (5%) incubator at 37 °C. Cell viability was assessed by using trypan blue exclusion.

Treatment of Cells With IL-6 and JAK-STAT Pathway Inhibitors

IgA1-secreting cells were plated at 1×10^5 cells/well in 24-well plates, treated with IL-6 (40 ng/ml) in the presence of the STAT3 inhibitor, Stattic (Tocris Biosciences, Bristol, UK) at final concentrations 0 to 10 μ M,

or with JAK inhibitor AZD1480 (LC Laboratories, Woburn, MA) (for peripheral blood mononuclear cell [PBMC]–derived cells, 0–2 μM ; for tonsil-derived cells, 0–300 nM). The cells were pre-incubated with inhibitor for 1 hour before addition of IL-6. Samples of culture medium were harvested after 5 days for analyses of total IgA1 and Gd-IgA1.

Determination of Total IgA1 Concentration

Total IgA1 was measured by enzyme-linked immunosorbent assay (ELISA).²⁸ Microplates coated with 0.1 μg /well of goat IgG F(ab')₂ specific for human IgA (Jackson ImmunoResearch Inc., West Grove, PA) were blocked with 1% bovine serum albumin (BSA) in phosphate-buffered saline (PBS) with 0.05% Tween 20 (PBS-T), washed, and incubated with serially diluted samples of cell-culture supernatants from IgA-producing cells, in conjunction with a standardized serum (Bio-Rad, Hercules, CA) for IgA quantification. Bound IgA was detected after addition of biotinylated goat IgG F(ab')₂ specific for human IgA (Biosource, San Diego, CA), followed by horseradish peroxidase (HRP)–conjugated Extravidin (Sigma, St. Louis, MO) and o-phenylenediamine dihydrochloride–hydrogen peroxide peroxidase substrate (Sigma). Optical densities were measured at 490 nm on an EL808 microplate reader (BioTek, Winooski, VT). As indicated previously, we cloned IgA-secreting cells and confirmed that the secreted IgA was exclusively IgA1; thus, we refer to it as total IgA1.²⁸

Gd-IgA1 Assay

Gd-IgA1 secreted in culture medium was measured by lectin ELISA.²⁸ Microplates coated with 0.25 μg /well of goat IgG F(ab')₂ specific for human IgA (Jackson ImmunoResearch Inc.) were blocked with 1% BSA in PBS-T, washed, and incubated with cell-culture supernatant added at 100 ng of IgA1 per well, and incubated overnight at 4 °C. Captured IgA1 was desialylated by neuraminidase (*Arthrobacter ureafaciens*; Glyko, Toronto, Ontario, Canada) at 2 mU/ml for 3 hours at 37 °C. Gd-IgA1 was detected using biotinylated lectin from *Helix aspersa* (Sigma; HAA), specific for terminal GalNAc, at 2 μg /ml in 1% BSA in PBS-T, followed by HRP-conjugated Extravidin and o-phenylenediamine dihydrochloride–hydrogen peroxide peroxidase substrate. Optical densities were measured at 490 nm. The Gd-IgA1 concentration was determined by interpolating the sample optical density of the individual to the optical density on the standard curve constructed using serially diluted Gd-IgA1 (Ale). Because the standard Gd-IgA1 myeloma protein is not entirely devoid of galactose, the expression of results in micrograms per milliliter does not precisely reflect the concentration of

Gd-IgA1 in the sera. Therefore, we expressed the results in units per milliliter. One unit of Gd-IgA1 was defined as 1 μg of this standard Gd-IgA1 myeloma protein.

Evaluation of Phosphorylation of STAT3

To evaluate STAT3 phosphorylation in individual cell lines treated with IL-6 and JAK-STAT inhibitors, cells were plated in 6-well plates at 1×10^6 cells/well and treated with different concentrations of AZD1480 or Stattic for 1 hour, followed by addition of IL-6 at a final concentration of 40 ng/ml for 15 minutes. Cell lysates were prepared for Western blot analyses using M-PER lysis buffer with a cocktail of phosphatase and protease inhibitors (Thermo Fisher Scientific, Waltham, MA). To determine the long-term effects of IL-6 treatment on phosphorylation of STAT3, EBV-immortalized, IgA1-producing cell lines derived from cells in the peripheral blood of IgAN patients (IgAN-PB cells) and HC (HC-PB cells) were exposed to IL-6 at a final concentration of 40 ng/ml for 1, 3, and 48 hours in the presence or absence of JAK inhibitor AZD1480 (0.3- or 2- μM concentration).

Sodium Dodecylsulfate–Polyacrylamide Gel Electrophoresis and Western Blot Analysis

IL-6- and JAK-STAT–treated cells were spun down, and the pellets were washed in ice-cold PBS and lysed in M-PER lysis buffer containing a protease inhibitor cocktail and a phosphatase inhibitor cocktail (Thermo Fisher Scientific). Cell debris was removed by centrifugation for 10 minutes at 14,000g at 4 °C. Protein concentrations in the supernatants were measured using a protein assay kit (Bio-Rad); aliquots corresponding to 7 μg /lane of total protein were separated by sodium dodecylsulfate–polyacrylamide gel electrophoresis and transferred to polyvinylidene difluoride membrane for Western blot analysis. After transfer, the membranes were blocked by Superblock (Thermo Fisher Scientific) and incubated with phospho-Y705-STAT3- or phospho-S727-STAT3–specific rabbit polyclonal antibodies, both diluted 1:800 in blocking buffer, or with STAT3-specific mouse monoclonal antibodies diluted 1:10,000 (R & D Systems, Minneapolis, MN). Bound antibodies were detected by addition of HRP-conjugated anti-rabbit (1:4000) or anti-mouse (1:10,000) IgG antibodies (Southern Biotech, Birmingham, AL), respectively, followed by addition of chemiluminescence substrate (Thermo Fisher Scientific), then visualized on Kodak radiography film (Kodak, Rochester, NY). Densitometric evaluation with ImageJ software (National Institutes of Health, Bethesda, MD; <https://imagej.nih.gov/ij/>) was used with *in vitro* titration of STAT3 in cellular lysates for calibration of densitometric curves.

Quantitative Real-Time Polymerase Chain Reaction Analysis

RNA was isolated from 2×10^5 cells using the RNeasy 96 Mini Kit (Qiagen, Hilden, Germany) and converted to cDNA by the SuperScript III First-Strand Synthesis SuperMix kit (Invitrogen, Carlsbad, CA). Levels of STAT3 and glyceraldehyde-3-phosphate dehydrogenase (GAPDH) transcripts were determined by real-time polymerase chain reaction (RT-PCR) using LightCycler 480 DNA SYBR Green I Master chemistry on LightCycler 480 instrument (Roche, Basel, Switzerland). Results were expressed as the fold change versus the result for the corresponding GAPDH housekeeping gene mRNA values using the $2^{-\Delta\Delta C_t}$ method.³¹

STAT3 siRNA Treatment

IgA1-producing cell lines derived from PBMCs from 3 patients with IgAN (IgAN-PB) and 3 HC-PB were transfected by ON-TARGETplus SMARTpool siRNAs (Thermo Fisher Scientific) specific for human STAT3. ON-TARGETplus nontargeting SMARTpool siRNAs served as a control. Cells were inoculated at a density of 5×10^5 /ml 24 hours before siRNAs were added. Before transfection, the cells were harvested by centrifugation for 10 minutes at 300g and resuspended at room temperature in Nucleofector Solution C (Lonza, Basel, Switzerland) at a density of 2.5×10^6 /100 μ l for each transfection. After addition of 1.4 μ g of individual siRNA, cells were pulsed in an Amaxa nucleofector II (Lonza) using program X-001 and then immediately transferred to a 24-well panel containing 1.4 ml of culture medium and incubated in humidified carbon dioxide incubator at 37 °C. Twenty-four hours after transfection, the knock-down efficiency was determined by RT-PCR. The knock-down effect was expressed as cDNA level of the individual gene normalized to GAPDH, after respective siRNA treatment, divided by respective value obtained after treatment by nontargeting siRNA.

Kinomic Profiling

Cell lysates from IgAN-PB and HC-PB cells ($n = 3$ for each) stimulated with 40 ng/ml of IL-6 were incubated without or with 1 μ M AZD1480 for 10 minutes immediately before kinomic analysis using high-throughput phosphopeptide microarrays. All analyses were performed in triplicate. Kinomic profiling was performed on cell lysates obtained by lysing 5×10^5 cells with M-PER lysis buffer as described in the section on Western Blotting Analysis and using the PamStation 12 platform (PamGene, 's-Hertogenbosch, Netherlands) in the UAB Kinome Core (www.kinomecore.com).^{32–34} After protein quantification by the bicinchoninic acid method (Thermo Fisher Scientific), lysates (12.5 μ g protein)

were loaded in kinase reaction buffer onto the Tyrosine-Kinase PamChip (PamGene). This platform uses a high-throughput peptide microarray system analyzing 144 individual tyrosine phosphorylatable peptides imprinted and immobilized in a 3-dimensional format to assess kinomic activity in cell lysates. Fluorescein isothiocyanate–conjugated anti-phosphotyrosine antibodies were used for visualization. Kinomic profiling data were analyzed using Evolve microarray software (PamGene). BioNavigator software (PamGene) was used for raw data transformation into kinetic (initial velocity) and steady-state (postwash) values across multiple exposure times. Significantly altered peptide lists (unpaired Student's *t*-test) were generated and uploaded to GeneGo MetaCore (portal.genego.com; Thompson Reuters, New York, NY) for network analysis, performed on September 5, 2012. Significantly altered peptide lists were cross compared for recurrent upstream kinases in Kinexus kinase predictor (www.phosphonet.ca), and scored according to recurrence and percent occurrence, as in our reports.^{33,34}

Statistical Analyses

Results were expressed as mean \pm SD (in some graphs, data are shown as means + SD for clarity). Data were analyzed using 2-tailed Student's *t*-test (unpaired or paired, as applicable). For analyzing multiple groups, 1-way analysis of variance was used, and $P < 0.05$ was regarded as significant.

RESULTS

IL-6 Increases Production of IgA1 and Gd-IgA1 in IgA1-Producing Cell Lines From IgAN Patients

EBV-immortalized, IgA1-producing cell lines derived from cells in peripheral blood IgAN patients (IgAN-PB cells) and HC (HC-PB cells) secreted comparable amounts of IgA1 into the culture medium under baseline conditions (Figure 1a). The IL-6–augmented production of IgA1 was not significantly different for IgAN-PB and HC-PB cells (Figure 1b). However, IgAN-PB cells secreted more Gd-IgA1 after IL-6 stimulation in comparison to the control cells (Figure 1c and d). We have also generated IgA1-producing cell lines from the tonsils of 2 patients with IgAN and 2 individuals with OSA, and performed exploratory experiments with these cells. IgA1-producing cell lines derived from the tonsils of patients with IgAN (IgAN-tonsillar cells) and individuals with OSA (OSA-tonsillar cells) secreted comparable amounts of IgA1 into the culture medium under baseline conditions (Supplementary Figure S1a and b), similar to the cell lines derived from the peripheral blood. Gd-IgA1 secretion by IL-6-stimulated, IgAN-tonsillar cells also increased, although statistical significance could not be

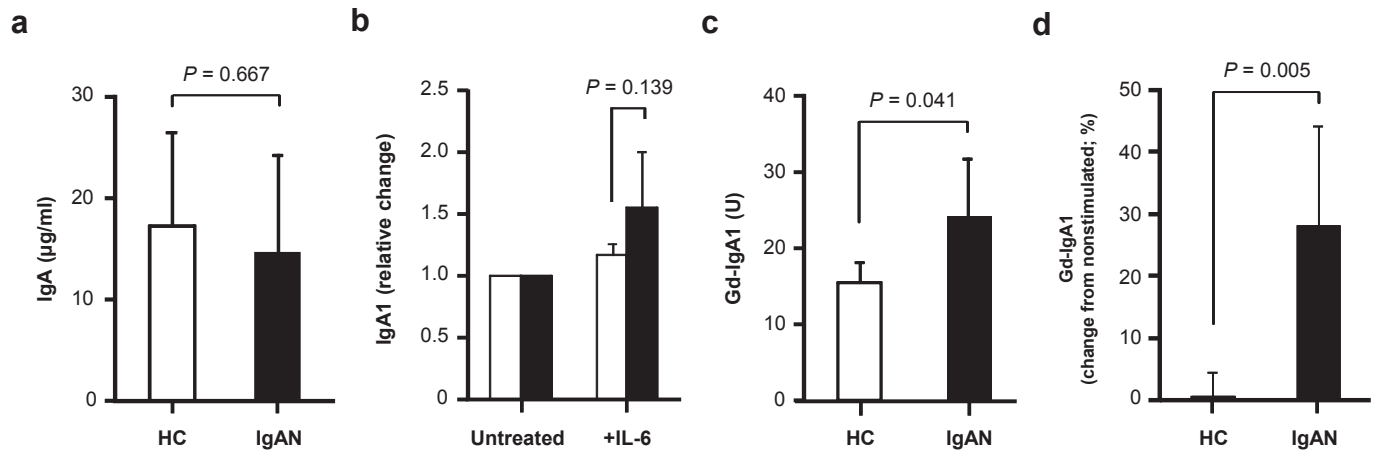


Figure 1. IgA1 and galactose-deficient (Gd)-IgA1 production by IgA1-secreting cells derived from Epstein-Barr virus–immortalized peripheral blood mononuclear cells from 5 healthy control subjects (HCs; white bars) and 5 IgA nephropathy (IgAN) patients (black bars) were stimulated with IL-6 (final concentration 40 ng/ml in all experiments) or mock-stimulated (untreated). (a) IgA1 concentration in the culture supernatant of IgA1-producing cells from HCs and IgAN patients. (b) IL-6 increased IgA1 production by IgA1-secreting cells from HCs and IgAN patients (by 16.9% for HCs and 55.8% for IgAN patients). (c) Gd-IgA1 secreted by IgA1-producing cells from HCs and IgAN patients. Cells from IgAN patients secreted more Gd-IgA1 compared with the cells from HCs (24.2 ± 7.5 U vs. 15.5 ± 2.7 U; values normalized to total IgA1). (d) IL-6 increased Gd-IgA1 production in cells from IgAN patients but not in HCs (relative change, $28.0 \pm 15.9\%$ vs. $0.0 \pm 4.2\%$). Mean values + SD from a representative experiment with 5 samples in each group.

calculated because there were only 2 subjects per group (Supplementary Figure S1c and d).

IL-6 Signaling Increases STAT3 Phosphorylation in IgA1-Secreting Cells of Patients With IgAN and HCs

In a pilot experiment performed with EBV-immortalized, IgA1-producing cell lines derived from PBMC from an IgAN patient and a HC, we tested whether the canonical STAT3 pathway was activated by IL-6. We found that IL-6 induced STAT3 phosphorylation at Y705, the STAT3 phospho-activation site, but not at S727 (the other site for transcriptional activation in STAT3) (Figure 2a–c). STAT3 phosphorylation at Y705 peaked at 15 minutes and was more pronounced in IgAN-PB cells than in HC-PB cells (Figure 2a and b). To confirm this difference for the phosphorylation at Y705, the experiment was repeated using IgA1-producing cell lines from 3 IgAN patients and 3 HCs. STAT3 phosphorylation at Y705 with IL-6 stimulation for 15 minutes was greater for the IgAN cell lines (Figure 2d and e). mRNA expression of the genes encoding the IL-6 receptor (*IL-6R1*, 2, and 3) in IgAN-PB and HC-PB cells did not reveal any significant differences. IL-6 stimulation did not alter mRNA levels of *IL-6R1*, 2, and 3 in IgA1-producing cell lines (data not shown).

STAT3 siRNA Knock-Down Blocks IL-6–Mediated Increase in Gd-IgA1 Production

STAT3 siRNA knock-down reduced *STAT3* mRNA expression by >90% in PBMC-derived cell lines from 3

IgAN patients and 3 HCs in comparison with mock-treated cells, as determined by quantitative RT-PCR analysis (Figure 3a). STAT3 protein levels were reduced in STAT3 siRNA-treated cells by >80% for both groups of cell lines (Figure 3b and c). Furthermore, the IL-6–induced increase in production of Gd-IgA1 in IgAN-PB cells was reduced by *STAT3* siRNA knock-down (Figure 3d). *STAT3* siRNA knock-down was associated with reduced total STAT3 protein and its phosphorylation at Y705 (Supplementary Figure S2a). IL-6–induced production of IgA1 in IgAN-PB cells was not altered by *STAT3* siRNA knock-down (Supplementary Figure S2b).

STAT3 Inhibitor, Stattic, Reduced IL-6–Induced STAT3 Phosphorylation, and Production of IgA1 and Gd-IgA1 in IgA1-Secreting Cell Lines From IgAN Patients

Stattic, a specific STAT3 inhibitor, decreased IL-6–induced production of IgA1 and Gd-IgA1 in IgAN-PB cells in a dose-dependent manner (Figure 4a and b). Stattic also reduced the IL-6–induced increase in production of Gd-IgA1 in IgAN-tonsillar cells (Supplementary Figure S3a and b). Stattic did not show a similar effect in PBMC- and tonsil-derived cells from control subjects. An inhibitory effect on production of IgA1 and Gd-IgA1 in PBMC-derived cells from IgAN patients and HCs was apparent at only the highest concentration of Stattic (10 μ M); this Stattic concentration reduced cell viability due to the toxicity of the inhibitor. In tonsillar cells from individuals with OSA,

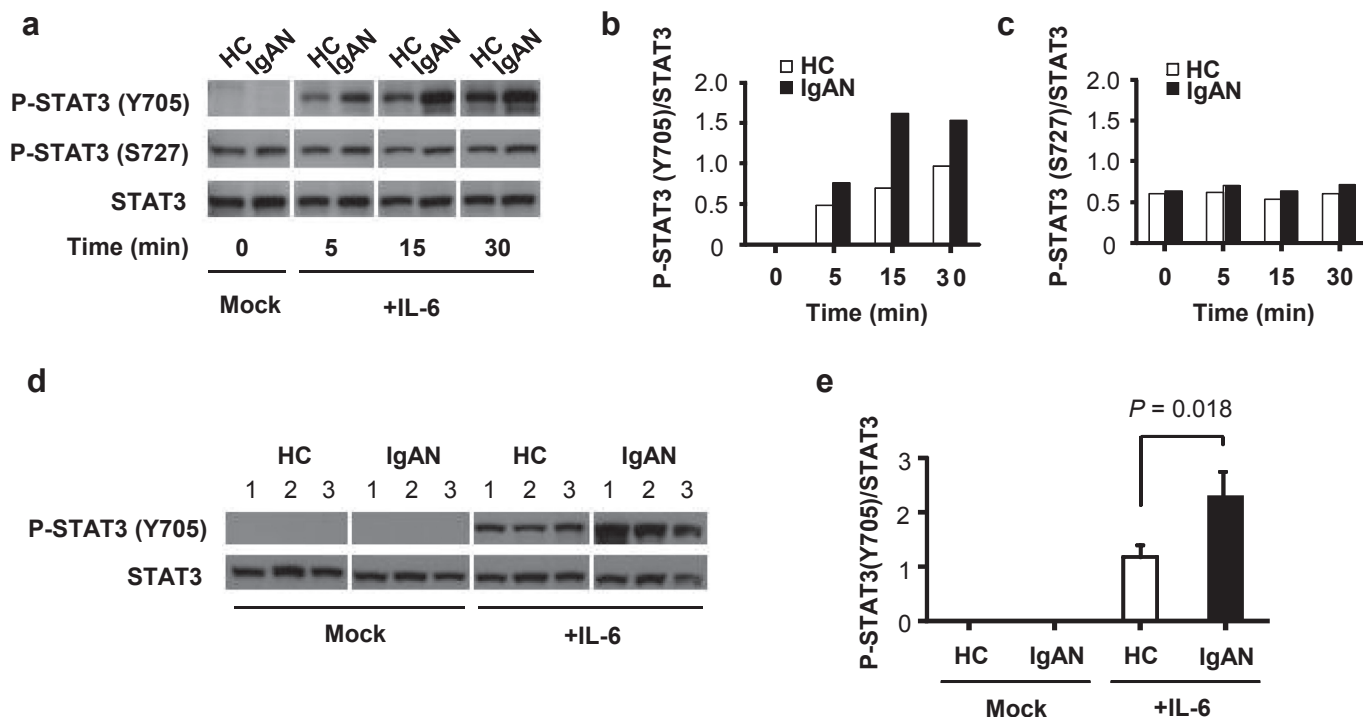


Figure 2. Interleukin-6 (IL-6)–induced STAT3 phosphorylation in IgA1-secreting cells. (a) Time course of IL-6–induced STAT3 phosphorylation (Y705 and S727) from IgA1-secreting cell lines derived from Epstein-Barr virus–immortalized peripheral blood mononuclear cells of 1 healthy control subject (HC) and 1 IgA nephropathy (IgAN) patient. Total STAT3 protein served as load control. This experiment was repeated using IgA1-producing cell lines from 3 IgAN patients and 3 HCs. Only a representative example is shown. (b,c) Densitometric analysis of P-STAT3 (Y705 and S727) levels relative to that of total STAT3 for blot in (a). (d) STAT3 phosphorylation (Y705) in IgA1-secreting cells from 3 HCs and 3 IgAN patients incubated for 15 minutes with or without IL-6. (e) Densitometric analysis of P-STAT3 (Y705) levels relative to that of total STAT3 for blot in (d). Representative blots are shown in (a) and (d) and mean values + SD from 1 experiment with 3 samples in each group are shown in (e).

10 μ M Stattic reduced production of IgA but had no apparent effect on Gd-IgA1. Stattic inhibited IL-6–induced STAT3 phosphorylation at Y705 in a dose-dependent manner in PBMC- and tonsil-derived cells from IgAN patients and in those from the control subjects (Figure 4c and d; Supplementary Figure S3c and d). Neither IL-6 nor Stattic had any effect on phosphorylation of STAT3 at S727 (data not shown).

JAK Inhibitor, AZD1480, Reduced IL-6–Induced STAT3 Phosphorylation, and Production of IgA1 and Gd-IgA1 in IgA1-Secreting Cell Lines From IgAN Patients

The JAK small molecule inhibitor, AZD1480, reduced the IL-6–induced increase in the production of IgA1 in IgAN-PB and HC-PB cells in a dose-dependent manner (Figure 5a). Moreover, AZD1480 inhibited the increased production of Gd-IgA1 induced by IL-6 in IgAN-PB cells (Figure 5b), with the maximal effect at a concentration of 2 μ M (Figure 5b). IgA1 production by IgAN-tonsillar and OSA-tonsillar cells was not inhibited by AZD1480 (Supplementary Figure S4a), but AZD1480 modestly inhibited increased production of Gd-IgA1 induced by IL-6 in IgAN-tonsillar cells (Supplementary Figure S4b).

AZD1480 inhibited IL-6–induced STAT3 phosphorylation at Y705 in the cells from IgAN patients (IgAN-PB and IgAN-tonsillar cells) and the control subjects (HC-PB and OSA-tonsillar cells) (Figure 5c and d, Supplementary Figure S4c and d).

IL-6 Induced Long-Lasting STAT3 Phosphorylation in IgAN-PB Cells; AZD1480 Inhibited This Effect

The IL-6-induced STAT3 phosphorylation at Y705 in IgAN-PB cells started to weaken after 1 hour, but was detected even after 48 hours (Figure 6a and b). In contrast, for HC-PB cells, this IL-6–induced phosphorylation was not long-lasting, and had dissipated by 3 hours (Figure 6a and b).

Kinomic Profiling Confirmed STAT-Signaling Pathways as the Main Target of AZD1480 Reducing the IL-6–Mediated Gd-IgA1 Overproduction

Kinomic profiling of IL-6–stimulated PBMC-derived cells from patients with IgAN versus those from HCs identified signaling pathways that were differentially inhibited by AZD1480. The cell lysates were treated *ex vivo* for 10 minutes with the inhibitor before the

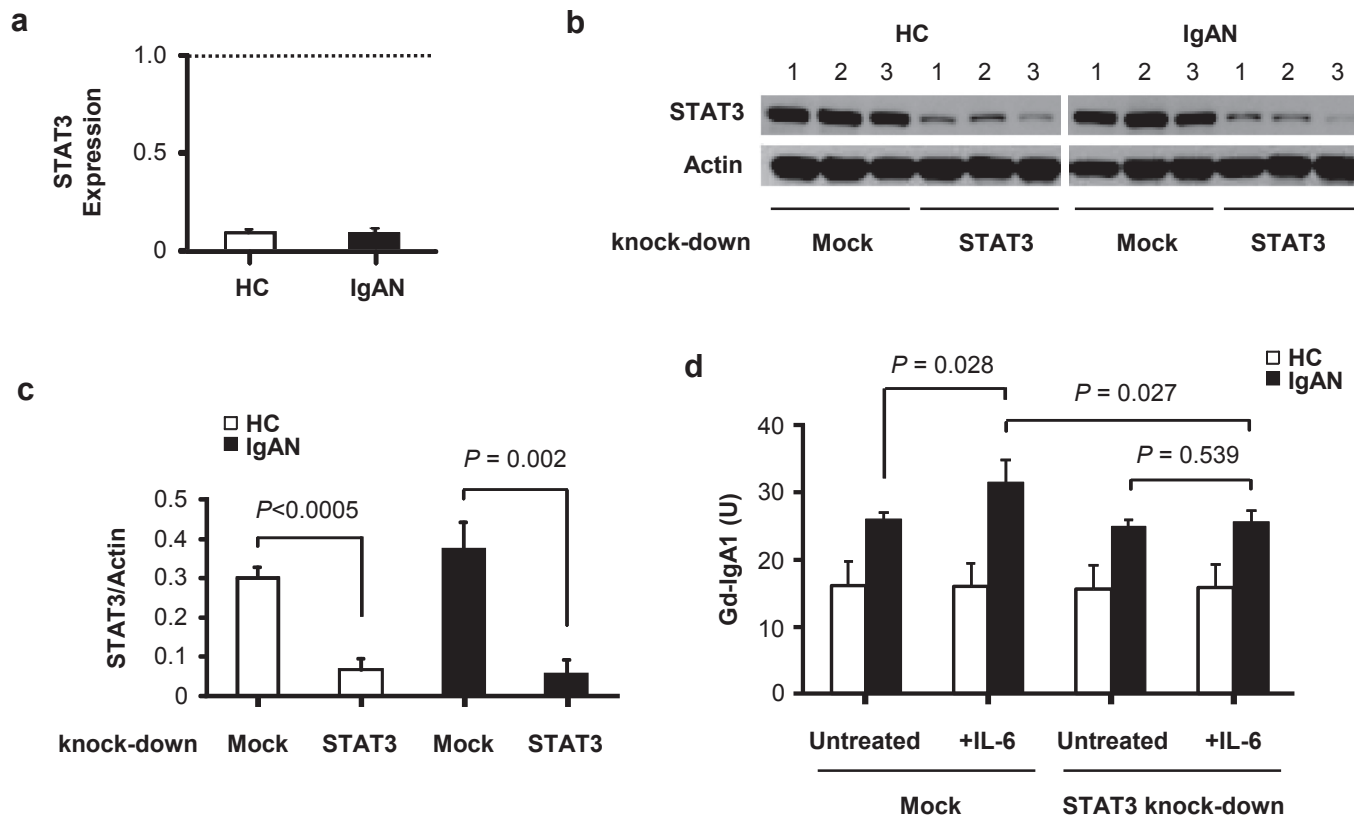


Figure 3. Expression of STAT3 is essential for overproduction of galactose-deficient IgA1 (Gd-IgA1) by IgA nephropathy (IgAN) cells in response to interleukin (IL-6). (a) Real-time polymerase chain reaction analysis of *STAT3* transcripts confirmed robust siRNA knock-down. Bars represent mean values + SD of knock-down in IgA1-secreting cell lines derived from peripheral blood mononuclear cells of 3 healthy control subjects (HCs) and 3 IgAN patients. *STAT3* transcript level in mock-control samples (transfection with nontargeting siRNA) was set to 1 for each cell type (i.e., HC, IgAN). (b) Reduction in STAT3 protein levels after siRNA transfection was confirmed by Western blotting. (c) Densitometric analysis of STAT3 protein levels relative to that of actin after siRNA transfection. (d) IL-6–induced overproduction of Gd-IgA1 in IgAN cells was blocked by *STAT3* siRNA knock-down. Mean values + SD are from a representative experiment with 3 samples in each group.

kinomic profiling. AZD1480 inhibited phosphorylation of 9 target peptides in the cells from patients with IgAN, whereas for the HCs, only a single peptide was inhibited in the lysates (and 2 were increased). Analysis by GeneGo MetaCore, canonical pathway mapping, and direct interactions mapping identified JAK/STAT and mitogen-activated protein kinase pathways as the highest ranked pathways (Table 1, Figure 7, Supplementary Figures S5 and S6, Supplementary Table S1). The JAK/STAT signaling pathway was previously identified as one of the top pathways enriched among the GWAS signals for IgAN (enrichment $P = 6.7 \times 10^{-14}$)²⁵. Thus, our kinomic profiling results provided orthogonal evidence for the involvement of this pathway in the pathogenesis of IgAN.

DISCUSSION

The frequent occurrence of macroscopic hematuria during upper respiratory tract infections in IgAN patients suggests a connection between mucosal

inflammation and kidney damage in these patients.^{17,22,35} In support of this connection, most Gd-IgA1 in circulating immune complexes is a polymeric form that is typically produced only at mucosal sites,³⁶ whereas most circulatory IgA1 is predominantly monomeric and produced in the bone marrow. Therefore, there is a possible connection between mucosal inflammation and increased synthesis of circulatory polymeric IgA1. There is limited information on the origin of Gd-IgA1–producing cells, but IgAN is now well characterized by the galactose deficiency of the IgA1 in the mesangial immunodeposits. This deposited Gd-IgA1 is likely derived from circulating immune complexes formed from Gd-IgA1 bound by Gd-IgA1–specific autoantibodies.^{9–11} Serum IgA1 in healthy individuals is believed to contain few or no galactose-deficient O-glycans, in contrast to that in IgAN patients.^{7,10,12–14,37} Why Gd-IgA1 is primarily in the polymeric form is unknown, whether as a byproduct of aberrant glycosylation itself or due to the mechanisms driving its production. Further

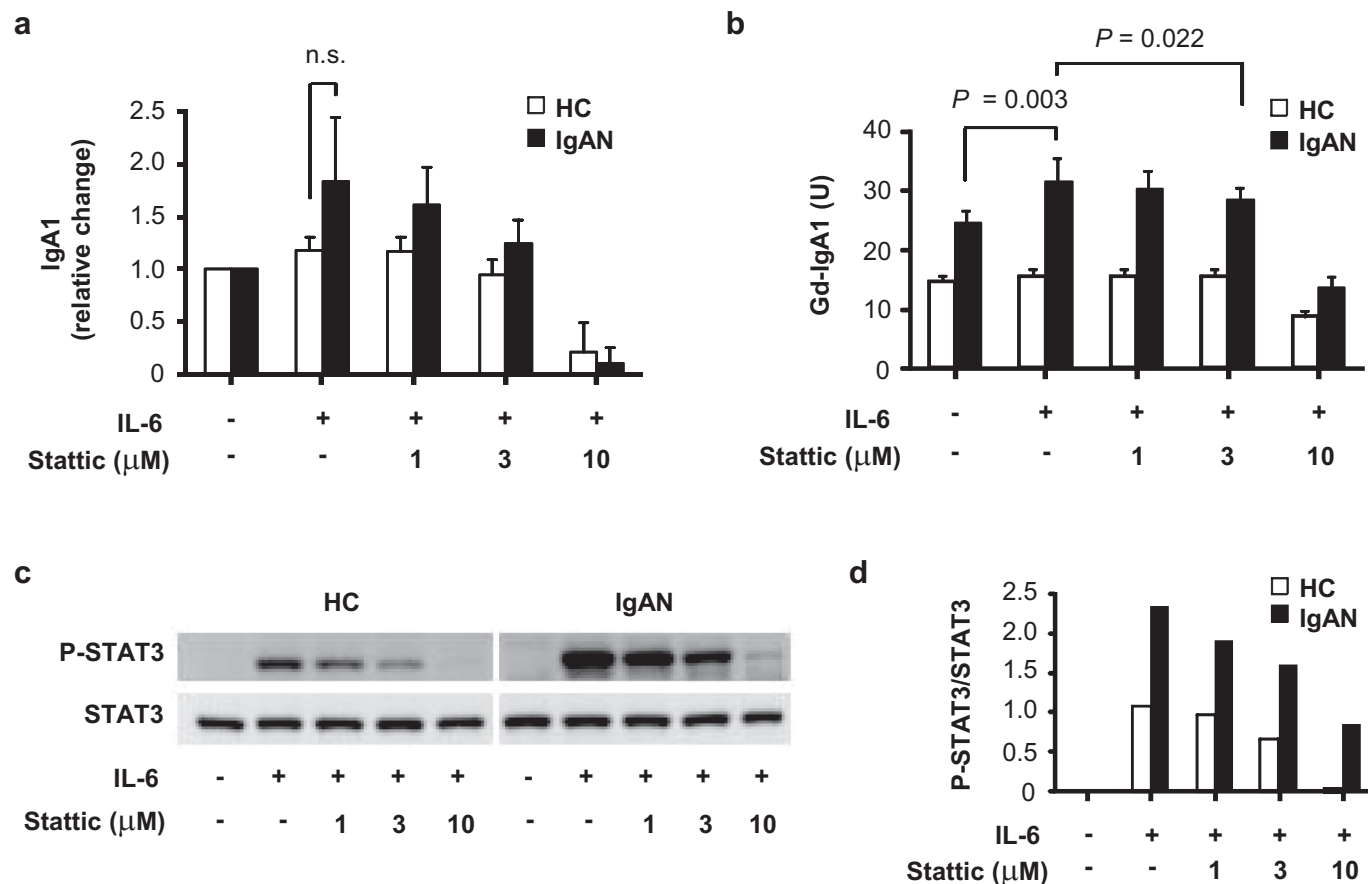


Figure 4. Static inhibits interleukin-6 (IL-6)-induced phosphorylation of STAT3 and overproduction of IgA1 and galactose-deficient (Gd)-IgA1 in IgA1-producing cells. IgA1-secreting cell lines derived from peripheral blood mononuclear cells of 3 healthy control subjects (HCs) and 3 IgA nephropathy (IgAN) patients were used. (a) Production of IgA1 and (b) Gd-IgA1 by IgA1-secreting cells from HCs and IgAN patients with IL-6 stimulation with and without Static pretreatment (1–10 μM). Mean values + SD from 1 representative experiment with 3 samples each are shown; $P = 0.003$ for comparison IL-6(-) versus IL-6(+), $P = 0.022$ for comparison 0 μM versus 3 μM Static. (c) Effect of Static inhibition on phosphorylation of Y705 STAT3 induced by IL-6 in HC or IgAN cells. One of 3 similar blots is shown. (d) Densitometric analysis of data from (c). Cell viability was $>90\%$ in HC and IgAN cells with Static pretreatment of 1 to 3 μM , but $<70\%$ in HC and IgAN cells with Static pretreatment of 10 μM , due to potential Static toxicity. Pretreatment with 10 μM of Static and follow-up IL-6 stimulation decreased cellular proliferation by $>70\%$ compared with that of untreated cells.

investigation into the origin of Gd-IgA1-producing cells may provide insights about environmental factors that affect aberrant glycosylation and may elucidate the connection between mucosal inflammation and kidney damage in IgAN patients. However, these studies are hampered by the lack of suitable experimental animal models, because only humans and hominoid primates have IgA1 with its O-glycans. Thus, alternative approaches must be used, such as IgA1-producing cells derived from the blood or tonsils of patients with IgAN and control subjects.

Elevated levels of circulatory Gd-IgA1 or Gd-IgA1-containing immune complexes in patients with IgAN have been correlated to disease progression or activity.^{16,17} This study showed how IL-6 mediates a significant effect on IgA1 glycosylation in cells of IgAN patients, but not in healthy individuals. IL-6 production is typically associated with activated,

cytokine-producing, T cells.³⁸ Thus, T cells have been implicated as a source of cytokines during mucosal infections, and as a contributor to the pathogenesis of IgAN.^{39–42} In addition, Th2 cytokine IL-4 may also play a role in controlling O-glycosylation of the IgA1 hinge region.⁴³ Although IL-4 did not elicit as much of an increase in Gd-IgA1 production from cells from IgAN patients as did IL-6, it is clear that O-glycosylation varies depending, in part, on the local cytokine milieu.^{26,27,43,44} Increased production of cytokines, such as IL-6, during mucosal inflammation may potentially explain clinical flares in IgAN patients that frequently coincide with common respiratory or gastrointestinal infections.

Across several ethnic backgrounds, serum Gd-IgA1 levels are a heritable trait.^{15,45,46} Asymptomatic blood relatives of IgAN patients frequently have significantly higher levels of Gd-IgA1 than do unrelated HCs,

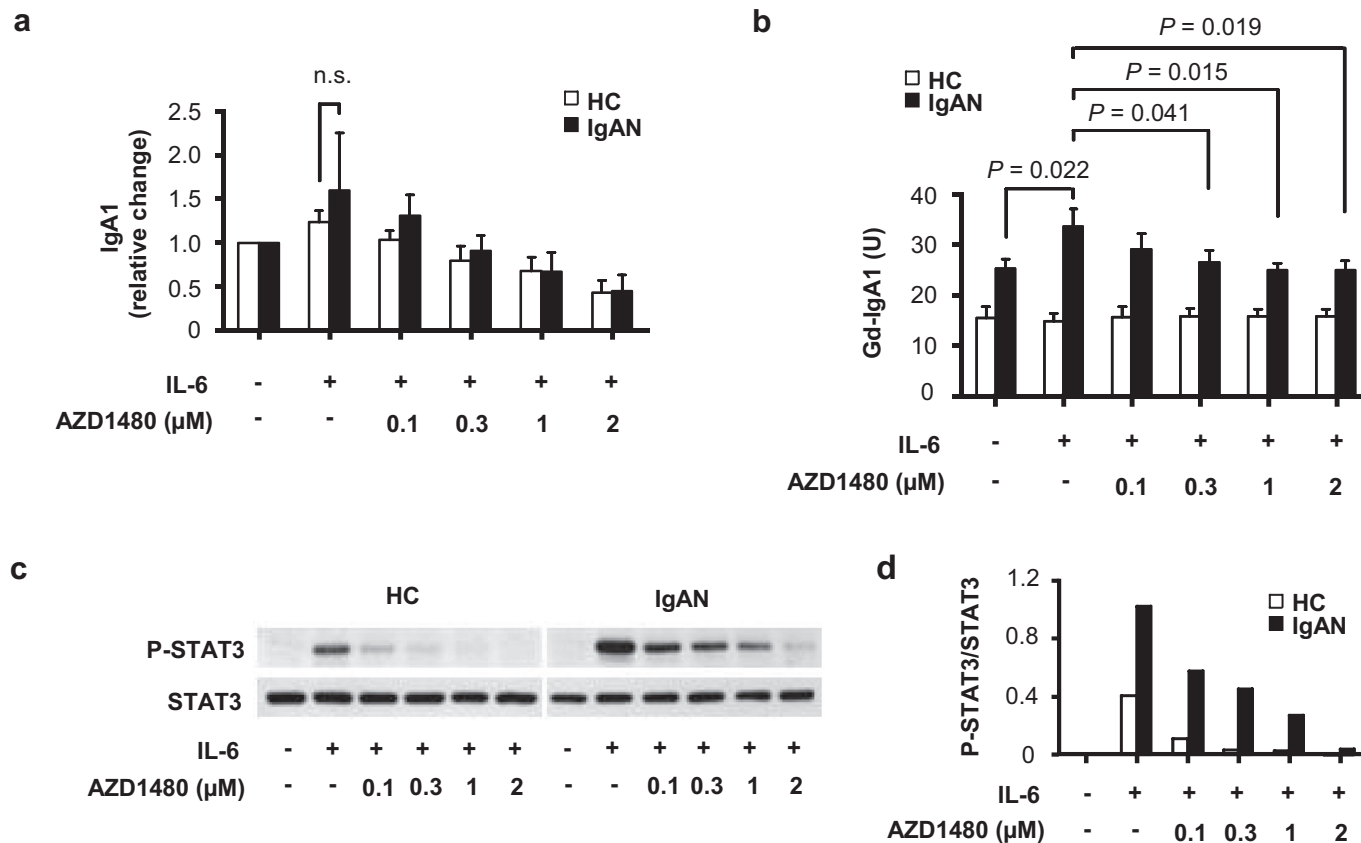


Figure 5. Effect of AZD1480 on phosphorylation of STAT3 and production of IgA1 and galactose-deficient (Gd-IgA1) by IgA1-secreting cells stimulated with interleukin-6 (IL-6). IgA1-secreting cell lines derived from peripheral blood mononuclear cells of 3 healthy control subjects (HCs) and 3 IgA nephropathy (IgAN) patients were used. (a) Production of IgA1 and (b) Gd-IgA1 by IgA1-secreting cells from HCs and IgAN patients after IL-6 stimulation with and without AZD1480 pretreatment (0.1–2 μM). Mean values + SD from 1 representative experiment with 3 samples each are shown. (c) Effect of AZD1480 on phosphorylation of Y705 STAT3 induced by IL-6 in HC or IgAN cells. One of 3 similar blots is shown. (d) Densitometric analysis of data from (c).

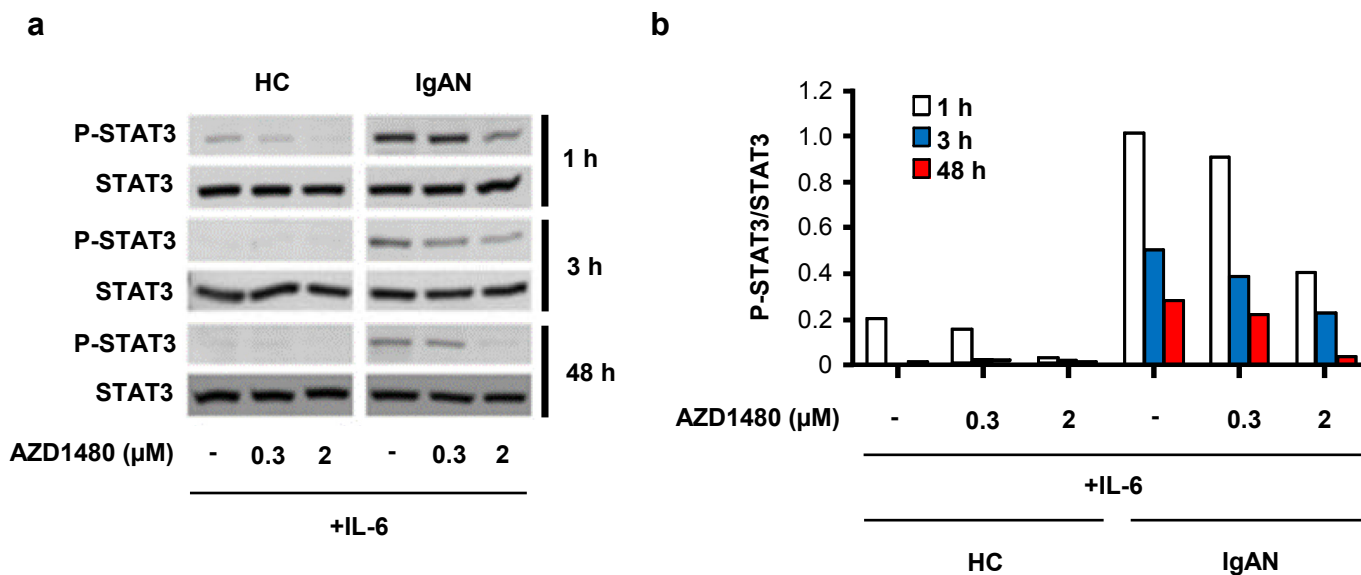


Figure 6. STAT3 activation by interleukin-6 (IL-6) was reduced by AZD1480 pretreatment. IgA1-secreting cell lines derived from peripheral blood mononuclear cells of 3 healthy control subjects (HCs) and 3 IgA nephropathy (IgAN) patients were used. (a) STAT3 Y705 phosphorylation was assessed 1, 3, and 48 hours after IL-6 stimulation with or without AZD1480 (0.3 or 2 μM). One of 3 similar blots is shown. (b) Densitometric analysis of data from (a).

Table 1. GeneGo MetaCore analyses identified pathways differentially inhibited by AZD1480 in interleukin-6–stimulated IgA1-producing cell lines derived from peripheral blood mononuclear cells from IgA nephropathy patients versus healthy-control subjects

GeneGo MetaCore canonical pathways	Hits	Possible	Corrected ratio
Development leptin signaling via JAK/STAT and MAPK cascades	3	4	0.75
Immune response IL-6 signaling pathway	3	4	0.75
Development VEGF-family signaling	4	6	0.67
G-protein signaling H-RAS regulation pathway	3	5	0.60
Development VEGF signaling and activation	3	5	0.60
Development VEGF signaling via VEGFR2-generic cascades	3	5	0.60
Development GDNF family signaling	3	6	0.50
Development EGFR signaling via small GTPases 7	3	7	0.43
Development CNTF receptor signaling	3	7	0.43
Development Angiopoietin-Tie2 signaling	3	7	0.43

CNTF, ciliary neurotrophic factor; EGFR, epidermal growth factor receptor; GDNF, glial cell derived neurotrophic factor; H-RAS, HRas proto-oncogene, GTPase; IL-6, interleukin-6; MAPK, mitogen-activated protein kinase; VEGF, vascular endothelial growth factor; VEGFR, VEGF receptor.

indicating that this abnormality is a necessary but not sufficient condition for development of IgAN.^{15,46} GWAS data support a genetic component, and recent reports have suggested that some stimuli, on a permissive genetic background, may cause low gene

expression of *C1GALT1* and *COSMC*, but enhanced gene expression of *ST6GALNAC-II*.^{28,47,48} The result of these 3 effects is reduced C1GalT1 activity and a lower content of galactose in the circulatory IgA1 in IgAN patients. The IL-6–enhanced aberrant glycosylation of IgA1 involves further dysregulation of expression and activity of C1GalT1 and ST6GalNAc-II in the cells from IgAN patients, leading to greater production of Gd-IgA1.²⁶ The association of *C1GALT1* and *COSMC* alleles with serum levels of Gd-IgA1 was revealed in a recent GWAS that confirmed the role of C1GalT1 in the production of Gd-IgA1.⁴⁹ Moreover, patients with IgAN have elevated levels of IL-6 in the circulation and locally in the kidneys.^{50–52}

IL-6 might play a crucial role in the pathogenesis of certain autoimmune and inflammatory diseases.⁵³ GWAS revealed a strong association of the genomic locus that encodes leukemia inhibitory factor and oncostatin M, 2 cytokines from the IL-6 family involved in mucosal immunity, with the risk of IgAN^{25,54} and inflammatory bowel disease.^{55,56} Differential activities of cytokines between patient and control cells highlighted either a change in signaling properties upstream or regulation of transcriptional activity downstream in controlling the glycosylation of

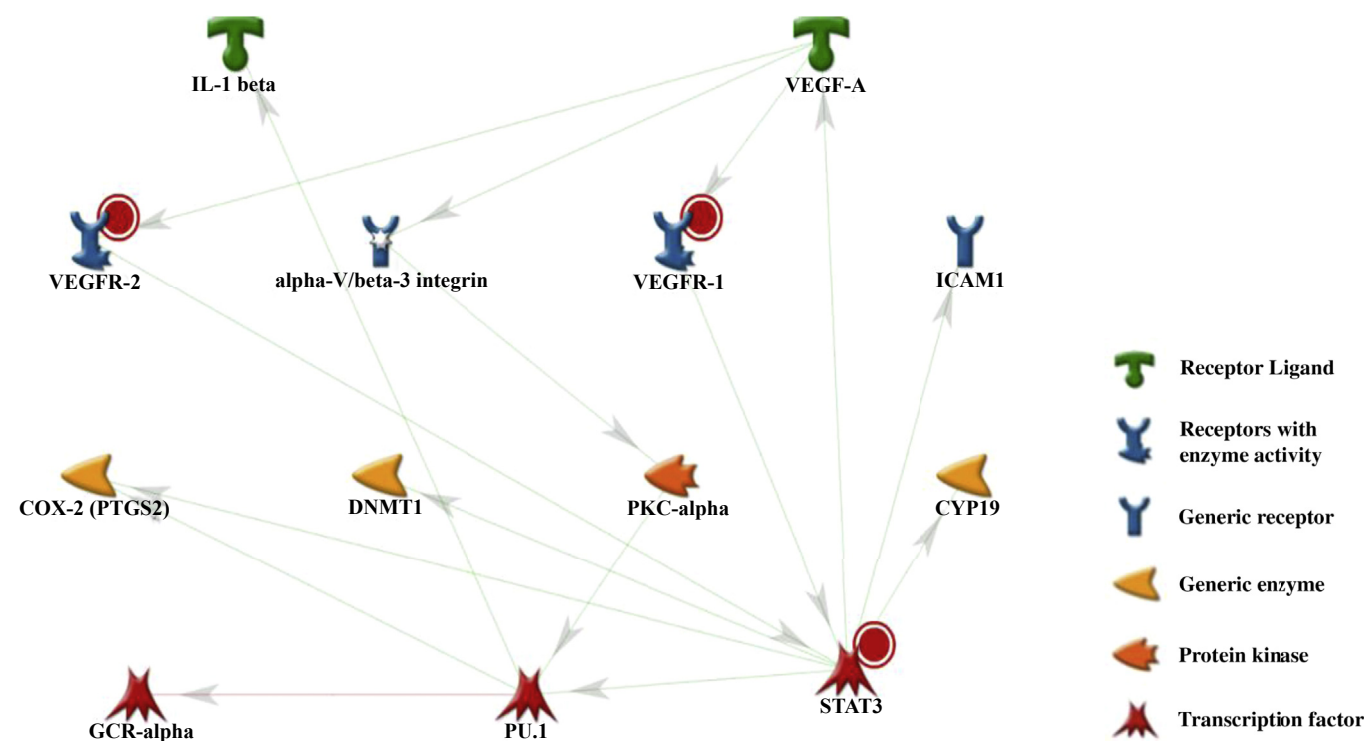


Figure 7. Kinomic profiling of IgA1-secreting cells from healthy control subjects (HC) and IgA nephropathy (IgAN) patients stimulated with interleukin-6 (IL-6) with or without the AZD1480 inhibitor. Direct interaction mapping using GeneGo MetaCore of phosphopeptides that were significantly inhibited by AZD1480-treated lysate from IgA1-secreting cells derived from peripheral blood mononuclear cells from patients with IgAN but not those from HCs, after IL-6 stimulation. In addition, a Build a Network modeling tool was used to generate likely interactions that link uploaded objects (significant phosphopeptides inhibited in the cell lysate from IgAN patients) similar to the known pathway models. Pathways representing vascular endothelial growth factor receptor (VEGFR) and STAT signaling axes were found and are displayed as the networks Signal transduction VEGF, STAT3 signaling (red circles).

IgA1. Consequently, multiple approaches are being developed and tested for therapeutic blocking of IL-6 activity.^{57,58}

We focused on the signaling mechanisms responsible for an IL-6–mediated increase in Gd-IgA1 production. We used IgA1-secreting cells derived from cells in peripheral blood and tonsils of patients with IgAN and control subjects without kidney disease. STAT3 phosphorylation is the classical signaling pathway associated with IL-6 signaling; therefore, we extended the approaches of other studies to analyze the level of STAT3 activation after IL-6 stimulation.^{59–61} The activation of STAT signaling pathways requires tyrosine phosphorylation of STAT proteins.⁶² In our study, IL-6 activation of STAT3 phosphorylation (Y705) was greater and persisted longer in IgA1-producing cells from IgAN patients compared with those from control subjects. The IL-6–induced increases in Gd-IgA1 production by IgA1-producing cells from IgAN patients were significantly reduced after siRNA *STAT3* knock-down. Small molecule inhibitors of the JAK/STAT3 pathway had varied efficacies in blocking IL-6–induced production of IgA1 in cells from IgAN patients and the control subjects, and in reducing production of Gd-IgA1 in IgAN cells. Kinomic analysis of tyrosine activation further validated the differential regulation of STAT3 signaling in IgAN cells compared with control cells. In addition, IgA1-producing, tonsil-derived cells from IgAN patients showed similarly enhanced Gd-IgA1 production and STAT3 activation in response to IL-6, which indicated the ubiquitous nature of dysregulated glycosylation of IgA1 in IgAN.

We analyzed 9 different STAT3 ChIP-seq datasets for B cells, to search for STAT3-binding sites close to any of the key glycosyltransferase genes involved in Gd-IgA1 production. We found upstream and downstream binding-site hits for the *CIGALT1* gene, which provided further insight into possible control of this gene mediated by IL-6/STAT3 signaling. Specifically, because the binding sites for transcription factor SP1/3 at the promoter of *CIGALT1* gene play an essential role in transcriptional regulation,⁶³ one can envision a negative regulatory effect by activated STAT3. This model would explain the previously observed down-regulation of *CIGALT1* transcription after IL-6 stimulation.²⁶

STAT3 signaling is a critical interface between autoimmunity and immune deficiency. Dominant negative mutations produce an immunodeficiency syndrome that results in hyper-IgE production, recurrent staphylococcal infections, and eczema, attributed to impaired IL-17 signaling in this disorder.^{64,65} Gain-in-function mutations in STAT3 produce autoimmunity with a high predisposition to type 1 diabetes, celiac disease, and

hematologic disorders.^{66–69} In these conditions and other diseases, treatment aimed at abnormal STAT3 signaling greatly ameliorated the symptoms.^{70,71}

In summary, an enhanced and extended IL-6–induced activation of STAT3 phosphorylation (Y705) represents a pathogenic process in IgAN that results in the overproduction of Gd-IgA1, the key pathogenic molecule in IgAN. Because there is no targeted therapy of IgAN, IL-6–mediated STAT3 signaling offers a promising area for investigation for treatment of this disease.

DISCLOSURE

BAJ and JN report that they are founding members of Reliant Glycosciences, LLC and had past sponsored-research agreements with Pfizer and Anthera and consulted for Visterra, Inc. HS, ZM, YS, RJW, YT, BAJ, and JN are co-inventors on US patent application 14/318,082 (assigned to UAB Research Foundation). All the other authors declared no competing interests.

ACKNOWLEDGMENTS

We thank the staff at the University of Alabama at Birmingham for the help with sample collection and storage. This study was supported in part by National Institutes of Health grants DK078244, DK082753, DK106341, DK105124, DK079337, and GM098539, by a gift from the IGA Nephropathy Foundation of America, and by grant number 15-33686A from Ministry of Health of the Czech Republic and IGA_LF_2017_009.

SUPPLEMENTARY MATERIALS

Figure S1. IgA1 and galactose-deficient (Gd)-IgA1 production by IgA1-secreting cells derived from the tonsillar tissues, with or without interleukin-6 (IL-6) stimulation.

Figure S2. Phosphorylation of STAT3 and IgA1 production in IgA1-producing cells after interleukin-6 (IL-6) stimulation with siRNA knock-down.

Figure S3. Effects of Stattic on phosphorylation of STAT3 and production of IgA1 and galactose-deficient (Gd)-IgA1 in IgA1-producing cells derived from the tonsillar tissues and stimulated with interleukin-6 (IL-6).

Figure S4. Effects of AZD1480 on phosphorylation of STAT3 and production of IgA1 and galactose-deficient (Gd)-IgA1 in IgA1-producing cells derived from the tonsillar tissues and stimulated with interleukin-6 (IL-6).

Figure S5. GeneGo MetaCore pathway map for development leptin signaling via JAK/STAT and mitogen-activated protein kinase (MAPK) cascades.

Figure S6. GeneGo MetaCore pathway map for immune response interleukin-6 (IL-6) signaling pathway.

Table S1. Phosphopeptides inhibited by AZD1480 after interleukin-6 stimulation in peripheral blood mononuclear cell–derived cells from IgA nephropathy patients.

Supplementary material is linked to the online version of the paper at www.kireports.org.

REFERENCES

- Berger J, Hinglais N. [Intercapillary deposits of IgA-IgG]. *J Urol Nephrol. (Paris)*. 1968;74:694–695.
- Julian BA, Waldo FB, Rifai A, et al. IgA nephropathy, the most common glomerulonephritis worldwide. A neglected disease in the United States? *Am J Med*. 1988;84:129–132.
- D'Amico G. Natural history of idiopathic IgA nephropathy: role of clinical and histological prognostic factors. *Am J Kidney Dis*. 2000;36:227–237.
- Conley ME, Cooper MD, Michael AF. Selective deposition of immunoglobulin A1 in immunoglobulin A nephropathy, anaphylactoid purpura nephritis, and systemic lupus erythematosus. *J Clin Invest*. 1980;66:1432–1436.
- Hiki Y, Kokubo T, Iwase H, et al. Underglycosylation of IgA1 hinge plays a certain role for its glomerular deposition in IgA nephropathy. *J Am Soc Nephrol*. 1999;10:760–769.
- Allen AC, Bailey EM, Brenchley PE, et al. Mesangial IgA1 in IgA nephropathy exhibits aberrant O-glycosylation: observations in three patients. *Kidney Int*. 2001;60:969–973.
- Suzuki H, Kiryluk K, Novak J, et al. The pathophysiology of IgA nephropathy. *J Am Soc Nephrol*. 2011;22:1795–1803.
- Wyatt RJ, Julian BA. IgA nephropathy. *N Engl J Med*. 2013;368:2402–2414.
- Suzuki H, Fan R, Zhang Z, et al. Aberrantly glycosylated IgA1 in IgA nephropathy patients is recognized by IgG antibodies with restricted heterogeneity. *J Clin Invest*. 2009;119:1668–1677.
- Tomana M, Matousovich K, Julian BA, et al. Galactose-deficient IgA1 in sera of IgA nephropathy patients is present in complexes with IgG. *Kidney Int*. 1997;52:509–516.
- Tomana M, Novak J, Julian BA, et al. Circulating immune complexes in IgA nephropathy consist of IgA1 with galactose-deficient hinge region and antiglycan antibodies. *J Clin Invest*. 1999;104:73–81.
- Allen AC, Harper SJ, Feehally J. Galactosylation of N- and O-linked carbohydrate moieties of IgA1 and IgG in IgA nephropathy. *Clin Exp Immunol*. 1995;100:470–474.
- Mestecky J, Tomana M, Crowley-Nowick PA, et al. Defective galactosylation and clearance of IgA1 molecules as a possible etiopathogenic factor in IgA nephropathy. *Contrib Nephrol*. 1993;104:172–182.
- Moldoveanu Z, Wyatt RJ, Lee JY, et al. Patients with IgA nephropathy have increased serum galactose-deficient IgA1 levels. *Kidney Int*. 2007;71:1148–1154.
- Gharavi AG, Moldoveanu Z, Wyatt RJ, et al. Aberrant IgA1 glycosylation is inherited in familial and sporadic IgA nephropathy. *J Am Soc Nephrol*. 2008;19:1008–1014.
- Zhao N, Hou P, Lv J, et al. The level of galactose-deficient IgA1 in the sera of patients with IgA nephropathy is associated with disease progression. *Kidney Int*. 2012;82:790–796.
- Coppo R, Basolo B, Martina G, et al. Circulating immune complexes containing IgA, IgG and IgM in patients with primary IgA nephropathy and with Henoch-Schoenlein nephritis. Correlation with clinical and histologic signs of activity. *Clin Nephrol*. 1982;18:230–239.
- Novak J, Tomana M, Matousovich K, et al. IgA1-containing immune complexes in IgA nephropathy differentially affect proliferation of mesangial cells. *Kidney Int*. 2005;67:504–513.
- Mestecky J, Raska M, Julian BA, et al. IgA nephropathy: molecular mechanisms of the disease. *Annu Rev Pathol*. 2013;8:217–240.
- Levy M, Gonzalez-Burchard G, Broyer M, et al. Berger's disease in children. Natural history and outcome. *Medicine*. 1985;64:157–180.
- Floege J, Feehally J. The mucosa-kidney axis in IgA nephropathy. *Nat Rev Nephrol*. 2016;12:147–156.
- Bene MC, Faure GC. Mesangial IgA in IgA nephropathy arises from the mucosa. *Am J Kidney Dis*. 1988;12:406–409.
- Xie Y, Chen X, Nishi S, et al. Relationship between tonsils and IgA nephropathy as well as indications of tonsillectomy. *Kidney Int*. 2004;65:1135–1144.
- Kiryluk K, Novak J, Gharavi AG. Pathogenesis of immunoglobulin A nephropathy: recent insight from genetic studies. *Annu Rev Med*. 2013;64:339–356.
- Kiryluk K, Li Y, Scolari F, et al. Discovery of new risk loci for IgA nephropathy implicates genes involved in immunity against intestinal pathogens. *Nat Genet*. 2014;46:1187–1196.
- Suzuki H, Raska M, Yamada K, et al. Cytokines alter IgA1 O-glycosylation by dysregulating C1GalT1 and ST6GalNAc-II enzymes. *J Biol Chem*. 2014;289:5330–5339.
- Smith AC, Molyneux K, Feehally J, et al. O-glycosylation of serum IgA1 antibodies against mucosal and systemic antigens in IgA nephropathy. *J Am Soc Nephrol*. 2006;17:3520–3528.
- Suzuki H, Moldoveanu Z, Hall S, et al. IgA1-secreting cell lines from patients with IgA nephropathy produce aberrantly glycosylated IgA1. *J Clin Invest*. 2008;118:629–639.
- Inoue T, Sugiyama H, Hiki Y, et al. Differential expression of glycogenes in tonsillar B lymphocytes in association with proteinuria and renal dysfunction in IgA nephropathy. *Clin Immunol*. 2010;136:447–455.
- Sato D, Suzuki Y, Kano T, et al. Tonsillar TLR9 expression and efficacy of tonsillectomy with steroid pulse therapy in IgA nephropathy patients. *Nephrol Dial Transplant*. 2012;27:1090–1097.
- Livak KJ, Schmittgen TD. Analysis of relative gene expression data using real-time quantitative PCR and the $2^{-\Delta\Delta C_T}$ method. *Methods*. 2001;25:402–408.
- Gilbert AN, Shevin RS, Anderson JC, et al. Generation of microtumors using 3D human biogel culture system and patient-derived glioblastoma cells for kinomic profiling and drug response testing. *J Vis Exp*. 2016:e54026.
- Anderson JC, Willey CD, Mehta A, et al. High throughput kinomic profiling of human clear cell renal cell carcinoma identifies kinase activity dependent molecular subtypes. *PLoS One*. 2015;10:e0139267.
- Anderson JC, Taylor RB, Fiveash JB, et al. Kinomic alterations in atypical meningioma. *Med Res Arch*. 2015;3, 10.18103/mra.v0i3.104.
- Le W, Liang S, Chen H, et al. Long-term outcome of IgA nephropathy patients with recurrent macroscopic hematuria. *Am J Nephrol*. 2014;40:43–50.

36. Boyd JK, Cheung CK, Molyneux K, et al. An update on the pathogenesis and treatment of IgA nephropathy. *Kidney Int.* 2012;81:833–843.
37. Mattu TS, Pleass RJ, Willis AC, et al. The glycosylation and structure of human serum IgA1, Fab, and Fc regions and the role of N-glycosylation on Fc α receptor interactions. *J Biol Chem.* 1998;273:2260–2272.
38. Diehl S, Rincon M. The two faces of IL-6 on Th1/Th2 differentiation. *Mol Immunol.* 2002;39:531–536.
39. Hurtado A, Johnson RJ. Hygiene hypothesis and prevalence of glomerulonephritis. *Kidney Int.* 2005;68(suppl 97):S62–S67.
40. Chintalacharuvu SR, Emancipator SN. The glycosylation of IgA produced by murine B cells is altered by Th2 cytokines. *J Immunol.* 1997;159:2327–2333.
41. Chintalacharuvu SR, Emancipator SN. Differential glycosylation of two glycoproteins synthesized by murine B cells in response to IL-4 plus IL-5. *Cytokine.* 2000;12:1182–1188.
42. Inoshita H, Kim BG, Yamashita M, et al. Disruption of Smad4 expression in T cells leads to IgA nephropathy-like manifestations. *PLoS One.* 2013;8:e78736.
43. Yamada K, Kobayashi N, Ikeda T, et al. Down-regulation of core 1 β 1,3-galactosyltransferase and Cosmc by Th2 cytokine alters O-glycosylation of IgA1. *Nephrol Dial Transplant.* 2010;25:3890–3897.
44. Royle L, Roos A, Harvey DJ, et al. Secretory IgA N- and O-glycans provide a link between the innate and adaptive immune systems. *J Biol Chem.* 2003;278:20140–20153.
45. Hastings MC, Moldoveanu Z, Julian BA, et al. Galactose-deficient IgA1 in African Americans with IgA nephropathy: serum levels and heritability. *Clin J Am Soc Nephrol.* 2010;5:2069–2074.
46. Lin X, Ding J, Zhu L, et al. Aberrant galactosylation of IgA1 is involved in the genetic susceptibility of Chinese patients with IgA nephropathy. *Nephrol Dial Transplant.* 2009;24:3372–3375.
47. Qin W, Zhou Q, Yang LC, et al. Peripheral B lymphocyte β 1,3-galactosyltransferase and chaperone expression in immunoglobulin A nephropathy. *J Intern Med.* 2005;258:467–477.
48. Malycha F, Eggermann T, Hristov M, et al. No evidence for a role of *cosmc*-chaperone mutations in European IgA nephropathy patients. *Nephrol Dial Transplant.* 2009;24:321–324.
49. Kiryluk K, Li Y, Moldoveanu Z, et al. GWAS for serum galactose-deficient IgA1 implicates critical genes of the O-glycosylation pathway. *PLoS Genet.* 2017;13:e1006609.
50. Rostoker G, Rymer JC, Bagnard G, et al. Imbalances in serum proinflammatory cytokines and their soluble receptors: a putative role in the progression of idiopathic IgA nephropathy (IgAN) and Henoch-Schönlein purpura nephritis, and a potential target of immunoglobulin therapy? *Clin Exp Immunol.* 1998;114:468–476.
51. Panichi V, Migliori M, De Pietro S, et al. C-reactive protein and interleukin-6 levels are related to renal function in predialytic chronic renal failure. *Nephron.* 2002;91:594–600.
52. Ranieri E, Gesualdo L, Petrarulo F, et al. Urinary IL-6/EGF ratio: a useful prognostic marker for the progression of renal damage in IgA nephropathy. *Kidney Int.* 1996;50:1990–2001.
53. Papanicolaou DA, Wilder RL, Manolagas SC, et al. The pathophysiologic roles of interleukin-6 in human disease. *Ann Intern Med.* 1998;128:127–137.
54. Gharavi AG, Kiryluk K, Choi M, et al. Genome-wide association study identifies susceptibility loci for IgA nephropathy. *Nat Genet.* 2011;43:321–327.
55. Imielinski M, Baldassano RN, Griffiths A, et al. Common variants at five new loci associated with early-onset inflammatory bowel disease. *Nat Genet.* 2009;41:1335–1340.
56. Liu JZ, van Sommeren S, Huang H, et al. Association analyses identify 38 susceptibility loci for inflammatory bowel disease and highlight shared genetic risk across populations. *Nat Genet.* 2015;47:979–986.
57. Anglesio MS, George J, Kulbe H, et al. IL6-STAT3-HIF signaling and therapeutic response to the angiogenesis inhibitor sunitinib in ovarian clear cell cancer. *Clin Cancer Res.* 2011;17:2538–2548.
58. Jones SA, Scheller J, Rose-John S. Therapeutic strategies for the clinical blockade of IL-6/gp130 signaling. *J Clin Invest.* 2011;121:3375–3383.
59. Bende RJ, Jochems GJ, Frame TH, et al. Effects of IL-4, IL-5, and IL-6 on growth and immunoglobulin production of Epstein-Barr virus-infected human B cells. *Cell Immunol.* 1992;143:310–323.
60. Lin L, Benson DM Jr., DeAngelis S, et al. A small molecule, LLL12 inhibits constitutive STAT3 and IL-6-induced STAT3 signaling and exhibits potent growth suppressive activity in human multiple myeloma cells. *Int J Cancer.* 2012;130:1459–1469.
61. Lue C, Kiyono H, McGhee JR, et al. Recombinant human interleukin 6 (rhIL-6) promotes the terminal differentiation of in vivo-activated human B cells into antibody-secreting cells. *Cell Immunol.* 1991;132:423–432.
62. Heinrich PC, Behrmann I, Haan S, et al. Principles of interleukin (IL)-6-type cytokine signalling and its regulation. *Biochem J.* 2003;374:1–20.
63. Zeng J, Mi R, Wang Y, et al. Promoters of human *Cosmc* and *T-synthase* genes are similar in structure, yet different in epigenetic regulation. *J Biol Chem.* 2015;290:19018–19033.
64. Al Khatib S, Keles S, Garcia-Lloret M, et al. Defects along the Th17 differentiation pathway underlie genetically distinct forms of the hyper IgE syndrome. *J Allergy Clin Immunol.* 2009;124:342–348,348.e1–5.
65. Milner JD, Brenchley JM, Laurence A, et al. Impaired T(H)17 cell differentiation in subjects with autosomal dominant hyper-IgE syndrome. *Nature.* 2008;452:773–776.
66. Baran-Marszak F, Boukhar M, Harel S, et al. Constitutive and B-cell receptor-induced activation of STAT3 are important signaling pathways targeted by bortezomib in leukemic mantle cell lymphoma. *Haematologica.* 2010;95:1865–1872.
67. Cheng F, Wang H, Horna P, et al. Stat3 inhibition augments the immunogenicity of B-cell lymphoma cells, leading to effective antitumor immunity. *Cancer Res.* 2012;72:4440–4448.

68. Koskela HL, Eldfors S, Ellonen P, et al. Somatic STAT3 mutations in large granular lymphocytic leukemia. *N Engl J Med.* 2012;366:1905–1913.
69. Vogel TP, Milner JD, Cooper MA. The ying and yang of STAT3 in human disease. *J Clin Immunol.* 2015;35:615–623.
70. Munoz J, Dhillon N, Janku F, et al. STAT3 inhibitors: finding a home in lymphoma and leukemia. *Oncologist.* 2014;19:536–544.
71. Forbes LR, Milner J, Haddad E. Signal transducer and activator of transcription 3: a year in review. *Curr Opin Hematol.* 2016;23:23–27.